Physica C 470 (2010) 897–900

Contents lists available at ScienceDirect

Physica C

journal homepage: www.elsevier.com/locate/physc

Irreversibility of the threshold field for dendritic flux avalanches in superconductors

A.J. Qviller [a,*], V.V. Yurchenko [a], K. Eliassen [a], J.I. Vestgården [a], T.H. Johansen [a], M.R. Nevala [b], I.J. Maasilta [b], K. Senapati [c], R.C. Budhani [c]

[a] Department of Physics and Center for Materials Science and Nanotechnology, University of Oslo, P.O. Box 1048, Blindern, 0316 Oslo, Norway
[b] Nanoscience Center, Department of Physics, University of Jyvaskyla, P.O. Box 35, FIN 40014, Finland
[c] Department of Physics, Indian Institute of Technology Kanpur, Kanpur 208 016, India

ARTICLE INFO

Article history:
Available online 4 March 2010

Keywords:
Thermomagnetic instability
Flux avalanches

ABSTRACT

Hysteretic effects are seen in the upper and lower threshold fields for the appearance of dendritic flux instabilities, first explained in Yurchenko et al. [Phys. Rev. B 76 (2007) 092504], in NbN-films. We have measured the threshold fields at increasing and decreasing applied fields at different temperatures and proposed a mechanism explaining how the hysteresis arises by analyzing the field profiles inside the sample.

1. Introduction

In type-II superconductors, an increasing applied magnetic field will result in penetration of magnetic vortices. The vortices are pinned to structural defects and the simplest possible model of the resulting state is the Bean model, where a superconducting slab is described by a single parameter, its maximum lossless current j_c [1]. Even a generalization of this model, where j_c is replaced by a field-dependent $j_c(B)$, is however only a first approximation to the dynamics of most actual superconducting films. Flux jumps, where large numbers of vortices are suddenly depinned and redistributed, are experimentally observed in several materials. These jumps are explained by thermomagnetic instability: vortex motion causes heat dissipation, the heat depins new vortices which are set in motion by the Lorentz force of the flowing supercurrent, possibly resulting in a positive feedback loop seen as a flux avalanche [2]. In several materials, including the NbN studied, the flux avalanches have a dendritic shape. The thermomagnetic instability has an onset at a lower threshold applied field, explained in [3]. The field dependance of the critical current explains the existence of re-entrant stability at an upper threshold field [4].

2. Sample

With pulsed laser ablation of a high-purity Nb-target in a 99.9996% N_2 environment, superconducting NbN-films were created on (100) MgO substrates. The laser used was a KrF excimer laser (248 nm) operated at 20 Hz and with an energy density of 5 J/cm^2 at the target surface. The samples have a thickness of $d = 280$ nm and $T_c = 15$ K. Further details about sample production and characterization can be found in [5]. Lithography was done in a $CHF_3 + O_2$ plasma to yield rectangular samples. For this article, a sample of width 2.4 mm and length 4.8 mm was measured.

3. Experimental setup

For investigating the flux penetration into the NbN-sample, magneto-optical imaging (MOI) based on the Faraday effect was used. A bismuth-substituted ferrite garnet film was placed on top of the sample to act as a Faraday rotator. The film was examined under a Leica reflected light polarizing microscope and images were captured with a RetigaExi camera. With external magnetic field applied from a pair of coils supplied by a Delta Elektronika power supply, the magnitude of the local field was visualized using crossed polarizers and a mercury lamp. A continuous helium-flow cryostat manufactured by Oxford Instruments was used to cool the sample. In order to later be able to extract quantitative values for the magnetic field inside the sample, the light intensity of the indicator film as a function of applied field was recorded at $T = 17$ K, which is above the sample T_c. The Faraday rotation is assumed to only have a weak temperature dependence in the range of measurements.

4. Flux distribution

In Fig. 1, a series of flux distributions typical of NbN-films at the temperatures of interest are shown. The sample had been zero-field cooled to $T = 5$ K and the applied field B was ramped up with steps $\Delta B = 0.85$ mT. At the lowest fields, a smooth penetration

* Corresponding author.
E-mail address: atleq@fys.uio.no (A.J. Qviller).

0921-4534/$ - see front matter © 2010 Elsevier B.V. All rights reserved.
doi:10.1016/j.physc.2010.02.066

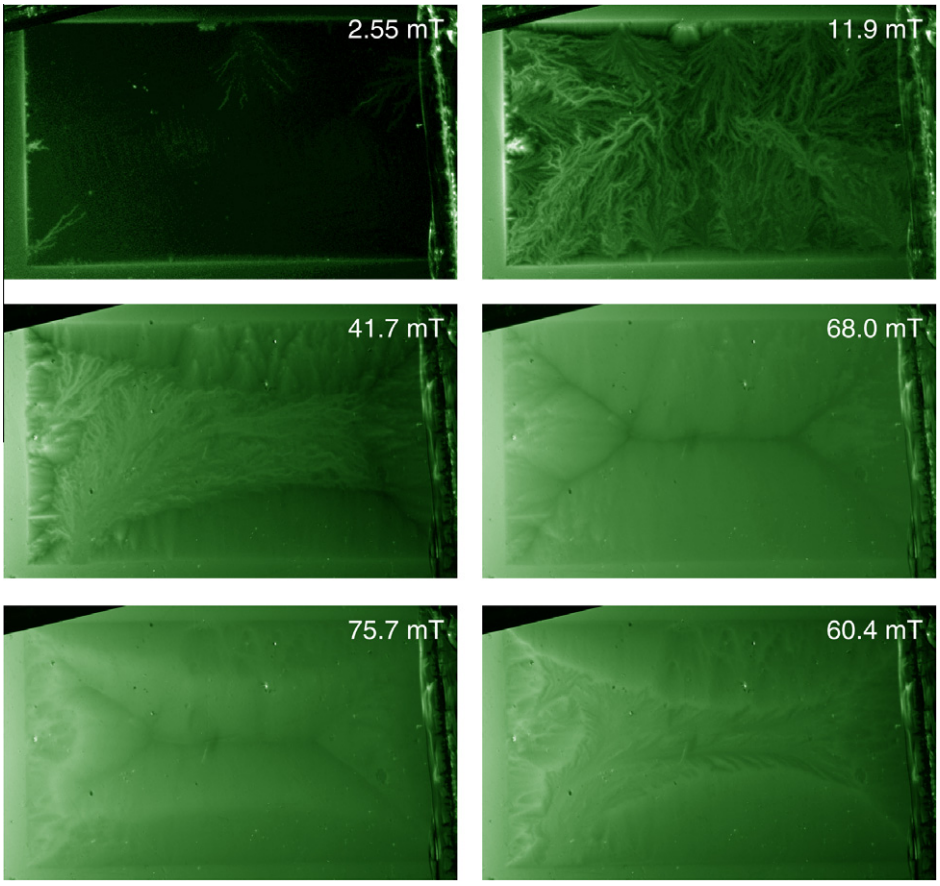

Fig. 1. Flux distributions at $T = 5$ K at different applied fields B.

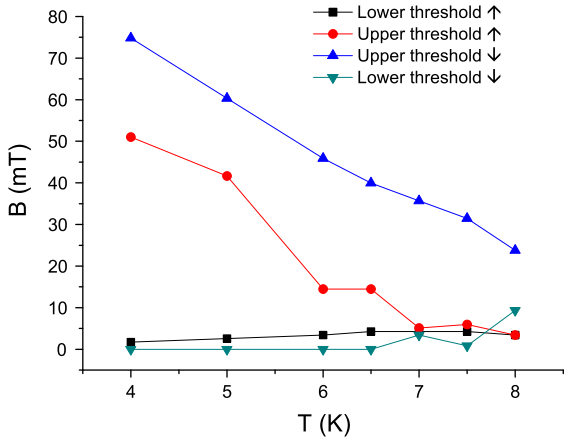

Fig. 2. Phase diagram showing threshold fields for thermomagnetic instability at increasing and decreasing fields as function of temperature. Maximum applied field is 85.0 mT, resolution 0.85 mT. Legend: ↑ = Ascending field, ↓ = Descending field.

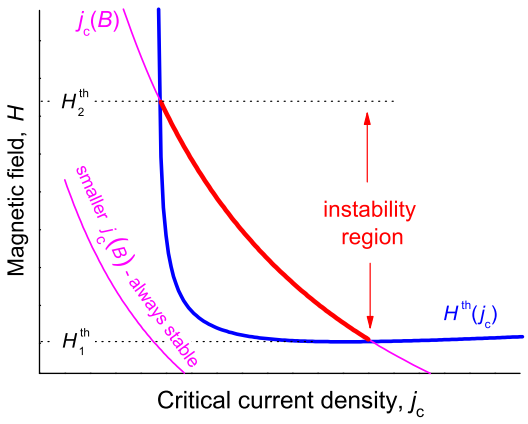

Fig. 3. Two threshold fields are defined by the intersection of $j_c(B)$ and $H^{th}(j_c)$.

similar to the Bean model was seen, but this regime ended at $B = 2.55$ mT, where the onset of thermomagnetic instability manifested itself as a flux avalanche appearing. At higher field $B = 11.9$ mT several more dendrites had appeared. The stability was regained at $B = 41.7$ mT and no new dendrites was seen at even higher fields. A Bean model like penetration pattern was instead gradually restored as shown in the image captured at $B = 68.0$ mT. After reaching the highest field ($B = 85.0$ mT, not shown), the field was decreased, initially without dendrites appearing. The image captured at $B = 75.7$ mT is representative of this Bean-model regime. At $B = 60.4$ mT, the first dendrite in descending field appeared. In the following, new dendrites were seen all the way down to $B = 0$ mT.

5. Phase diagram of thermomagnetic instability

Flux distributions at increasing and decreasing applied fields in the interval of temperatures from $T = 4$ K to $T = 10$ K were measured, and regimes of thermomagnetic instability and stability were recorded. The results are shown in Fig. 2. It is seen that for

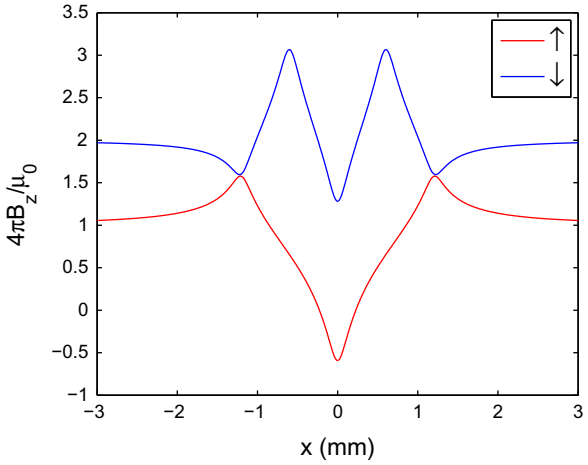

Fig. 4. Increasing (↑) and decreasing (↓) applied magnetic field profiles across the 2.4 mm wide sample centered at $x = 0$. Schematic drawing.

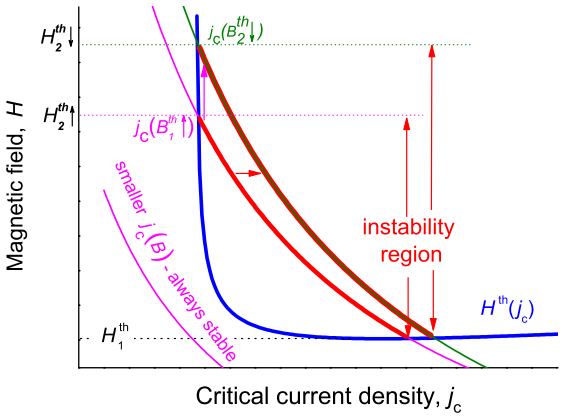

Fig. 5. Modification of Fig. 3 in order to take into account the internal field profiles from Fig. 4.

all measured temperatures in the interval between 4 K and 8 K, there is a substantial hysteresis in the upper threshold fields for increasing and decreasing applied field, while the lower threshold fields are closer, but not exactly identical. In order to explain the hysteresis, a recapitulation of the theory from [4] explaining re-entrant thermomagnetic stability is required. At low critical currents, the threshold field cannot be reached and the superconductor is stable against avalanches. But at higher critical currents, there will be lower and upper threshold fields for the instability, as seen in Fig. 3. The critical current decreases as the temperature rises towards T_c, such that the upper and lower threshold fields will converge towards the always-stable regime, as seen in Fig. 3. In order to extend the model from [4], the magnetic field profiles inside the superconductor are considered. They are obtained from direct integration of Biot–Savart's law and are shown schematically in Fig. 4 for the special case of the Bean model (field independent j_c). As the

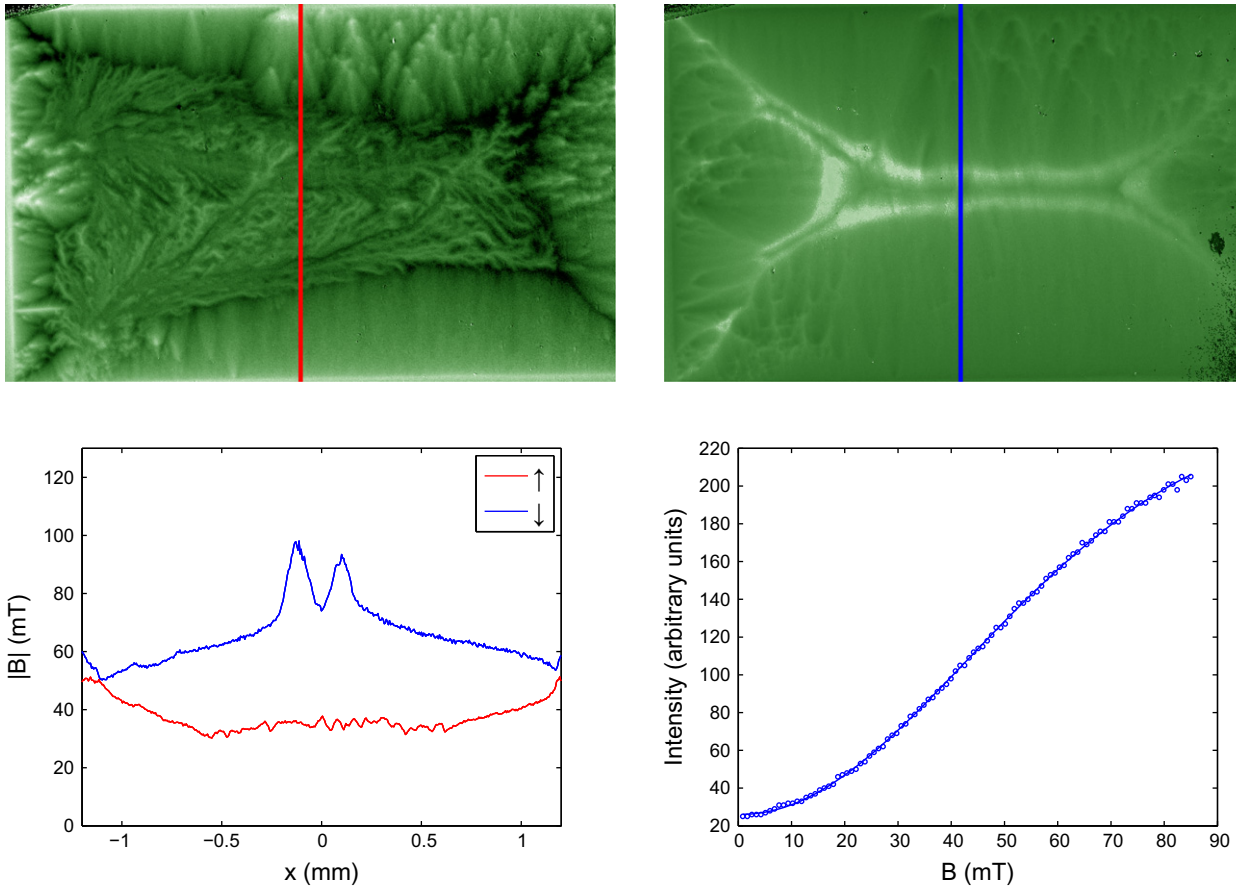

Fig. 6. Field distributions with transverse profiles. Upper left: before the last dendrite in increasing fields. Upper right: before the first dendrite in decreasing fields. Lower left: (↑ = Increasing field, ↓ = Decreasing field). Lower right: intensity calibration data with fit for a single pixel.

applied field is increased from zero, magnetic flux builds up just outside the film, sketched as the red[1] graph in Fig. 4. Inside the superconductor, the local field value depends on the critical current, which itself generally is a function of temperature and field and results from a self-consistent solution. The avalanches are formed close to the edges of the samples and therefore the important parameter is the local field in this region. As the sample is fully penetrated and the applied field is decreased, the currents close to the edges will reverse direction, resulting in minima in the field profile near the edges and sketched as the blue graph in Fig. 4. Thus, at a higher applied field at decreasing fields, the local field at the edge of the superconducting film is numerically similar to a lower applied field at increasing fields due to the different field profiles in increasing and decreasing fields. The critical current has generally a monotonic field dependence and will thus also have similar values at the edges for different applied fields, causing hysteresis in threshold fields for dendrite nucleation. Fig. 3 must therefore be modified to account for a higher critical current at the edge of the sample in decreasing applied fields compared to increasing applied fields and the result is seen in Fig. 5. The upper threshold fields differ substantially when this modification of the model is made and a higher upper threshold are seen at decreasing applied fields than at increasing applied fields. On the other hand, in this particular sample, the lower threshold field changes very little with increasing and increasing fields, as seen in Fig. 2.

6. Field profiles

The field profiles inside the sample had to be reconstructed, in order to experimentally check whether the hysteresis in the upper threshold field collapses when the local field at the edge of the sample instead of the applied field is examined, and thus confirm the above hypothesis. In order to do this, the magneto-optical images were calibrated. This was done by extracting the light intensity $I(x, y)$ response of the indicator film as a function of the applied $B_z(x, y)$ above T_c of the superconductor. For each pixel, the measured intensity was fitted to the light response function of the indicator film, given by Jooss et al. [6]. When the intensity function of all pixels in the image was obtained, intensity images $I(x, y)$ of the superconducting phase below T_c were solved for $B_z(x, y)$ by using the previously obtained coefficients. Transverse slices of this picture, showing field profiles, were extracted. This was done at the image before the last dendrite appearing in increasing fields and before the first dendrite appearing in decreasing fields. Slices were obtained at all temperatures in the interval between $T = 4$ K and $T = 8$ K, corresponding to Fig. 2. In Fig. 6 the profiles measured at $T = 5$ K are plotted. The magnetic fields at the edges are seen to be nearly equal, even if the externally applied fields differ substantially (Fig. 1). These results are representative of the measurements at the other temperatures.

7. Conclusion

It was hypothesized that the observed hysteresis in the threshold fields for the appearance of dendritic flux instabilities in superconducting NbN was caused by a combination of the different internal field profiles in increasing and decreasing fields together with the existence of upper and lower threshold fields for the onset of thermomagnetic instability. In this model, different applied fields gives rise to identical local fields. A magneto-optical investigation of an NbN-sample provides clear evidence that the local field at the edge of the sample is the parameter that matters for triggering dendritic flux instabilities.

Acknowledgment

This work was supported by the Norwegian Research Council Grant No. 158518/431 (NANOMAT).

References

[1] C.P. Bean, Rev. Mod. Phys. 36 (1964) 31.
[2] R.G. Mints, A.L. Rakhmanov, Rev. Mod. Phys. 53 (1981) 551.
[3] D.V. Denisov, D.V. Shantsev, Y.M. Galperin, E.-M. Choi, H.-S. Lee, S.-Ik. Lee, A.V. Bobyl, P.E. Goa, A.A.F. Olsen, T.H. Johansen, Phys. Rev. Lett. 97 (2006) 077002.
[4] V.V. Yurchenko, D.V. Shantsev, T.H. Johansen, M.R. Nevala, I.J. Maasilta, K. Senapati, R.C. Budhani, Phys. Rev. B 76 (2007) 092504.
[5] K. Senapati, N.K. Pandey, R. Nagar, R.C. Budhani, Phys. Rev. B 74 (2006) 104514.
[6] Ch. Jooss, J. Albrecht, H. Kuhn, S. Leonhardt, H. Kronmuller, Rep. Prog. Phys. 65 (2002) 675.

[1] For interpretation of color in Figs. 2–6, the reader is referred to the web version of this article.